



Dominik Schmid · Nils Gräbner · Utz von Wagner

# Friction-induced noise in drum brakes: finite-element modeling and experiments with special focus on damping

Received: 7 February 2022 / Accepted: 16 May 2022 / Published online: 13 June 2022  
© The Author(s) 2022

**Abstract** Brake squeal in friction brakes is a typical audible noise phenomenon in vehicles leading to high development and sometimes warranty costs for the suppliers. The friction forces generated during braking are responsible for self-excited vibrations in the audible frequency range starting from 1 kHz. In the past countermeasures against friction-induced vibrations are mostly investigated for disk brakes while the present study focuses on drum brakes. Damping is in the context of self-excited vibrations often one of the key measures. Nowadays recuperative braking in electric vehicles relieves the conventional friction brake. Due to safety reasons, electric vehicles need to possess at least a second independent brake system. Therefore, simpler drum brakes are on the rise again when developing brake systems. Compared to brake disks, where damping elements can hardly be implemented, the freely accessible drum surface and the brake shoes offer so far unused potential for applying passive damping measures. The present paper focuses on how damping measures influence the noise behavior of drum brakes. Industrial and non-industrial brake components are investigated in detail. Experimental as well as numerical procedures are used to assess damping and noise characteristics.

**Keywords** Drum brake · Brake squeal · Finite-element · Damping · Shim · Complex eigenvalue analysis

## 1 Introduction

Brake vibrations are a typical example of NVH problems in the automotive industry. The abbreviation Noise, Vibration, Harshness (NVH) describes undesired comfort-related mechanical dynamic phenomena that are noticeable or audible. Costs for development processes of automotive brakes are nowadays dominated by optimization with respect to the NVH behavior.

Most brake vibration phenomena are caused by self-excitation based on the friction forces between pad and disk or drum. Low frequency noise phenomena like creep groan are in general related to stick-slip phenomena between the contact partners, while high-frequency noise like squeal is (at least macroscopically) a pure sliding phenomenon. Fluctuating normal forces can nevertheless result in energy transfer from the rotation of the disk into vibrations, see e.g. [61]. Brake squeal is a high frequency noise phenomenon in the audible frequency

---

D. Schmid (✉) · N. Gräbner · U. von Wagner  
Chair of Mechatronics and Machine Dynamics (MMD), Technische Universität Berlin, Einsteinufer 5, 10587 Berlin, Germany  
E-mail: dominik.schmid@tu-berlin.de

N. Gräbner  
E-mail: nils.graebner@tu-berlin.de

U. von Wagner  
E-mail: utz.vonwagner@tu-berlin.de

range between 1 and 15 kHz [34]. Squealing automotive brakes are usually not accepted by customers. They result in high costs for warranty adjustments and, in order to avoid this, high effort in developing silent brakes. In [67] it is described that 60% of all brake-related warranty cases in the automotive sector is brake noise in the high-frequency range.

This kind of noise problem also occurs with other brake assemblies apart from disk brakes. In the past, drum brake systems largely disappeared from streetscape in passenger cars. However, this brake type is currently returning on the subject of electro mobility and particle emission. Generally drum brakes in modern cars are applied within the rear-axels [5], in addition to buses and trailers [28]. E-vehicles are in wide operational states decelerated using the recuperation principle in addition to conventional friction brakes. As a result classical braking systems are no longer permanently exposed to wear. Therefore, often simpler drum brakes are taken into account at least for rear-axles, still fulfilling the required braking characteristics.

The advantages of the drum brake speak for themselves [8]. The lower costs [23], the more robust design, the reduction of abrasion emissions due to the encapsulated design [60] and the significant weight advantage compared to disk brakes result in a longer range for electric vehicles. But nevertheless noise issues remain during the braking process, particularly before standstill. Drum brakes consist of a drum rotated during driving and two brake shoes being responsible for the deceleration of the vehicle. The shoes are either actuated by hydraulic wheel brake cylinders or using leverage mechanics acting as overrun brake in trailers.

However, remedial measures against friction-induced brake vibrations have been so far less intensively investigated for drum brakes but have to be taken into account in the future. According to [28], most of the research and development done for achieving silent brakes concentrate on disk brakes. Therefore to the best knowledge of the authors damping in drum brakes is widely not examined so far. Passive damping devices attached to brake shoes have already been examined in [1], but there hasn't been investigations regarding the set-up and positioning of damping devices to increase the damping level. Damping the outer drum using a ring damper has been presented in [65]. Investigations regarding damping effects in FE drum brake models are investigated for commercial automotive applications in [6,20].

A detailed literature research on the topic brake squeal can be found in [13,34,51]. Some common measures that have been introduced for reducing brake squeal in disk brakes are structural modifications like shifting of natural frequencies of brake components to prevent mode coupling [21]. Furthermore, in disk brakes mode coupling scenarios occur when modes of the brake system merge at the same natural frequency [36,42]. Often the geometry of the lining is adjusted by using chamfers or slots [3] as well as increasing the stiffness of essential parts [47,57] or reducing the rotational symmetry by adding additional masses [27,28]. Generally speaking the modal density of drum brakes is higher than in disk brakes [27,28]. This circumstance rather complicates the optimization of structural and vibration characteristics. Thus, the idea of decoupling frequencies which merge into a new mode shape turns out to be a difficult task.

Other measures for preventing squeal are active noise control like dither as described in [58] and applying passive damping structures [1]. Active measures for noise suppression can be very effective [18] but are associated with high tuning effort, costs and additional weight [14]. Therefore, the success is rather seen in the implementation of passive damping structures.

One aspect that is important in self-excited systems and promises remedy is providing a high dissipation level. Additional damping introduced in friction brakes can help to avoid high-frequency noise as described in [26]. The focus of this contribution is therefore more to highlight how damping in drum brake systems can be modeled and how it influences the stability behavior. It is obvious by comparing both brake principles—disk and drum—that the brake drum itself and the brake shoes offer sufficient potential to apply measures. Compared to drum brakes, in disk brakes there is much less space for applying damping solutions. This is mostly done on pad back plates. One of the key aspects, as done in [51], for disk brakes is to increase the damping of the drum itself [23]. The drum with its large surface is the main part for sound radiation such as squeal [27,42] and freely accessible for applying additional damping measures. Additionally to the already mentioned advantages, this could be a significant benefit for using drum brakes.

Often composite structures, called shims in the automotive industry, consisting of elastic and viscoelastic layers work particularly according to the constrained-layer-damping (CLD) principle. These composites are attached to pad back plates in disk brakes to increase the damping [2,48].

Due to a deformation of the shim and carrier structure elastomer layers are sheared resulting in an increase of damping. These CLD-structures can also be applied on brake shoes in drum brakes as well to increase the damping [28]. This additional damping source increases the damping of the whole brake shoe significantly.

An other aspect of this paper is how the simulation techniques developed for disk brakes are applicable to drum brakes. Hence, a fundamental Finite-element (FE) model is built up to be able to classify the influence of

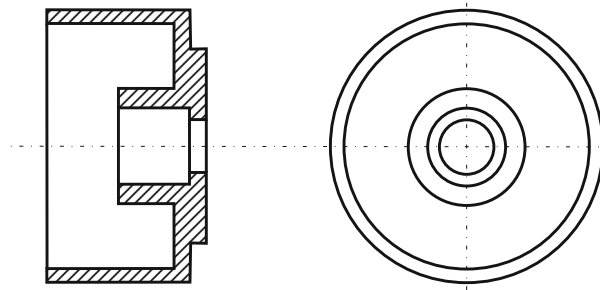


**Fig. 1** Non-industrial steel drum used for research purposes [52]

damping measures on drum brakes and to gain general experience with regard to simulation. Usually complex eigenvalue analysis (CEA) of high-dimensional FE disk brake models possessing a million or more degrees of freedom are carried out, e.g. [19,46]. These analyses are often run in the absence of damping, see [4] or focusing on shifting natural frequencies of brake components rather than increasing damping, like the altering of the chemical composition of the casting material [23].

Damping ratios of brake components will be carried out using experimental modal analyses. These dissipation characteristics are implemented in a simple FE drum brake model. It is investigated how damping and the location can influence the noise behavior.

## 2 Experimental investigations of drum brake components

Generally speaking drum brakes in passenger cars or trailers can be designed as simplex or duplex brakes depending on the use case and costs [10].<sup>1</sup> In simplex brakes there is one trailing and one leading shoe leading to either self-reinforcement or self-enhancement depending on the rotation direction. However, duplex drum brakes possess two leading shoes achieving a much greater braking effect due to self-reinforcement of both brake shoes in forward drive. Modeling simplex and duplex drum brakes in Finite-element models can be easily done by changing the force application and bearing point. Industrial brakes are often optimized in such way that there are almost no squealing events occurring in academic test series. Therefore, a steel drum manufactured at the chair's workshop instead of industrial gray cast iron ones is used for all investigations presented here. The simpler structure neglecting cooling fins also simplifies the FE modeling. The steel drum with an outer diameter of 214 mm has been turned from a hollow steel cylinder and is shown in Fig. 1.

Usually drums consist of cast material possessing a high damping potential among other suitable mechanical properties [23]. The focus in this contribution is how additional damping structures influence the overall damping behavior starting from a very low dissipation level. Therefore, it seemed suitable to use a steel drum having a lower damping potential compared to cast materials. For increasing the dissipation of the drum shims are applied. These shims are composite structures consisting of steel and elastomer layers [7,33,41]. Figure 2 shows schematically the principle of this composition.

The three-layer structure consists of a beam being significantly thicker than the additional layers involved in the composite, a thin viscoelastic intermediate layer (elastomer) and a rigid top layer. The soft viscoelastic core is sheared due to deformation of the whole compound. The damping increase is derived through internal friction processes [24] from converting mechanical energy mostly into heat [43,56].

The shims used for all investigations are industrial ones applied in the context of disc brake systems. The composition is shown in Fig. 2. Both elastomer coatings (NBR80) possess a thickness of 0.117 mm, the steel layer (G90) acting as constraining layer has a thickness of 0.406 mm and the adhesive (silicone) shows a thickness of 0.076 mm [51,66]. Dynamic mechanical analysis procedures have already been performed to determine the shim elastomer loss factor, the storage as well as loss modulus in the squeal relevant frequency range. The elastomer storage modulus is in the range between 80,000 and 100,000 MPa and the corresponding loss factor determined lies in the range 0.09 and 0.13. Detailed information describing the corresponding three point bending tests can be found in [50,51].

Modal analyses were carried out, inter alia in a student thesis [17] for an industrial drum brake. Therein components, i.e. the cast drum and the brake shoe, were investigated in its original version and after hav-

<sup>1</sup> There is a much greater variety of drum brakes like the Duo-Duplex drum brake, which is not the focus of this contribution.

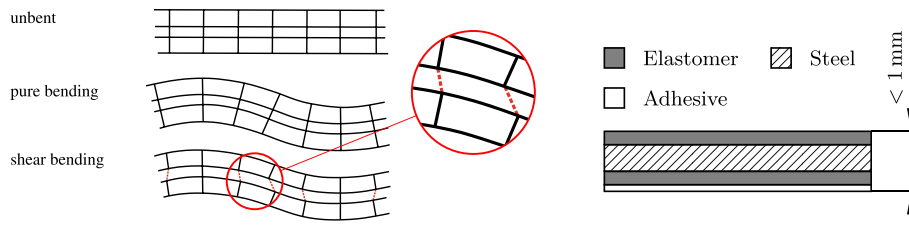


**Fig. 2** Constrained-layer-damping mechanism, [49,51] and shim structure used for the investigations according to [51,66], (Fig. 2.2b)

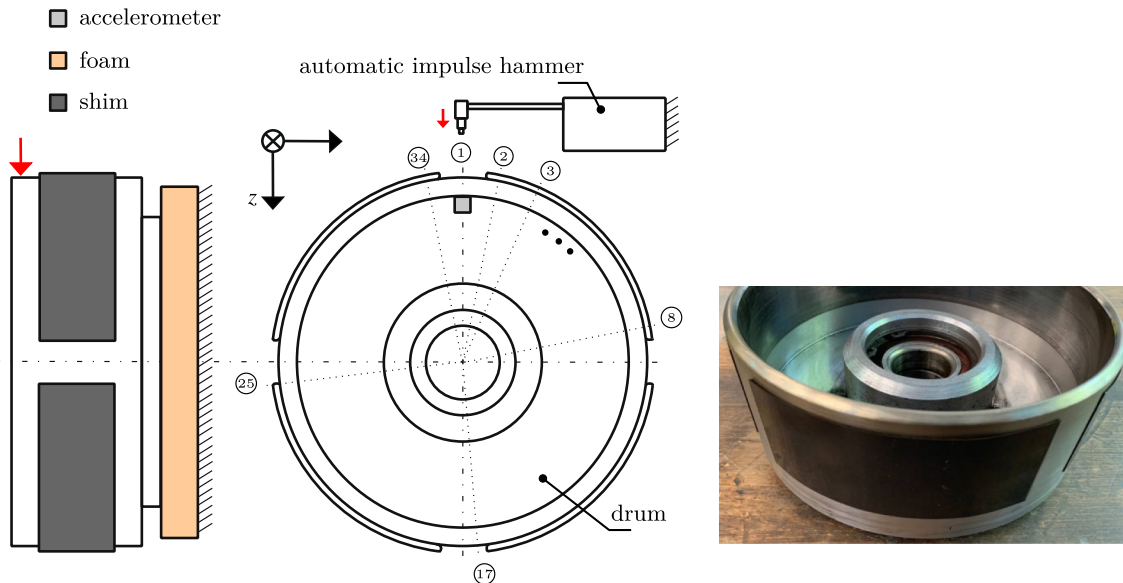


**Fig. 3** Modal analysis set-up of drum considering 34 collocation points [53] and real configuration

ing attached shim elements in several configurations. Finally in [17] also the mounted complete brake was examined. The results from [17] for the brake shoes are used here for the modeling while additional modal analyses were carried out for the academic steel drum. The results from [17] for the cast drum are used for comparison with the respective results from the academic steel drum. For increasing the drum damping four rectangular shim plates (width 53 mm, length 139 mm) are glued equidistantly along the circumference of the steel drum. Natural frequencies, damping characteristics as well as mode shapes are used for validating the developed Finite-element model. For the investigations of the academic steel drum, 34 collocation points along the circumference shown in Fig. 3 are provided for mapping high frequency mode shapes properly. For exciting the measurement object an automatic modal hammer (Maul-Theet, vImpact-60) is applied achieving force levels of approximately 30 N. As excitation area the steel part of the drum marked with a red arrow in Fig. 3 is used. An accelerometer (PCB 356A33) glued to the inner diameter of the drum at point 1 measures the radial system response ( $z$ -direction). The drum thereby is placed on soft foam for realizing a free-free support.

Frequency response functions (FRF) for the academic steel drum are recorded for 34 points in the frequency range up to 10 kHz. Figure 4 illustrates FRFs for points 1 and 25. Black FRFs show the drum configuration whereas red represent FRFs measured for the drum with shims. Measuring FRFs ten averages are considered. A multi-degree of freedom fitting mechanism for determining modal parameters is used [15]. Comparing both FRFs there is a significant reduction of resonance amplitudes as well as an expansion of the peaks visible when attaching shims to the outer drum surface. This suggests that the damping has been increased due the shim application.

How shims influence the modal behavior of the academic steel drum is shown in Tables 1 and 2. For classifying the results, damping ratios for steel are usually in the range of 0.0001 ... 0.001, polymers show ratios of 0.1 and larger [59]. Taking a closer look at Table 1 there is a slight shift in natural frequencies  $f$  visible due to the additional mass and stiffness added.

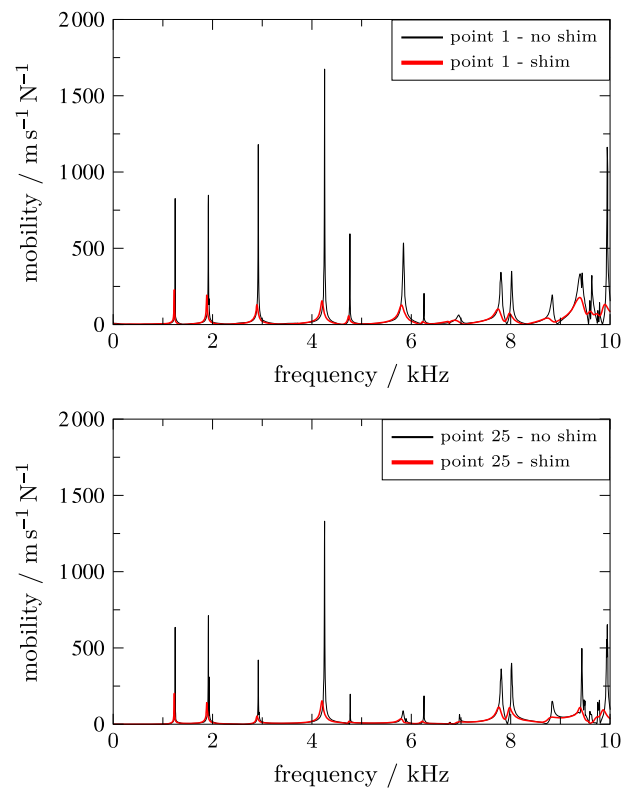


**Fig. 4** Frequency response functions of investigated drum at collocation points 1 and 25

**Table 1** Natural frequencies of academic steel drum

	$f_1$ Hz	$f_2$ Hz	$f_3$ Hz	$f_4$ Hz	$f_5$ Hz	$f_6$ Hz	$f_7$ Hz	$f_8$ Hz	$f_9$ Hz
No shim	1247	1914	2918	4252	4761	5839	6251	7799	8013
With shim	1230	1883	2892	4199	4731	5794	–	7730	7949

**Table 2** Damping ratios of academic steel drum

	$\vartheta_1$ %	$\vartheta_2$ %	$\vartheta_3$ %	$\vartheta_4$ %	$\vartheta_5$ %	$\vartheta_6$ %	$\vartheta_7$ %	$\vartheta_8$ %	$\vartheta_9$ %
No shim	0.057	0.070	0.079	0.061	0.030	0.210	0.019	0.232	0.135
With shim	0.252	0.424	0.703	0.632	0.351	0.841	–	0.831	0.568
Increase	342	506	790	936	1070	300	–	258	320

**Table 3** Properties of the industrial cast drum from [17]

Natural frequency in Hz	811	1902	3213	3301	5407	5827	7121	7150
Damping ratio in %	0.09	0.08	0.10	0.06	0.03	0.05	0.04	0.03

Damping ratios  $\vartheta$  for both drum set-ups are shown subsequently. As already assumed, adding shims results in an increase in damping caused by the constrained-layer-damping mechanism. Damping ratios are about 3 to 10 times larger than in the original steel drum.

For comparison, the results of the industrial cast drum obtained in [17] are given in Table 3. These investigations showed damping ratios of the industrial cast iron drum in the range of 0.03–0.10%.

A second suitable place to attach passive damping structures like shims is the brake shoe [1, 28]. Different attachment options have been tested in [17] varying the length, attachment place and the quantity of shims.



**Fig. 5** Industrial brake shoe attached with shims as investigated in [17]

**Table 4** Natural frequencies and damping ratios of brake shoes, results from [17]

	$\vartheta_1$   $f_1$ %   Hz	$\vartheta_2$   $f_2$ %   Hz	$\vartheta_3$   $f_3$ %   Hz	$\vartheta_4$   $f_4$ %   Hz	$\vartheta_5$   $f_5$ %   Hz	$\vartheta_6$   $f_6$ %   Hz
No shim	0.5 1431	0.7 2301	0.7 3148	0.9 3383	0.7 4334	1.3 5162
(a) 2 shims	–	0.9 2434	1.1 3210	0.7 3519	0.8 4432	2.0 5272
(b) 4 shims	0.9 1412	1.4 2296	1.6 3135	2.1 3392	1.4 4294	–

One of the thereby investigated shim placement options on an industrial brake shoes is visible in Fig. 5. Two variants that have shown the biggest impact on damping in [17] are: (a) two shims possessing measurements of  $125 \times 20 \text{ mm}^2$  similar to Fig. 5 and (b) four smaller shims ( $50 \times 20 \text{ mm}^2$ ) that are glued symmetrically to the brake shoe edges.

Since there is a strong mode shape dependency on system properties, it is very important to know which vibration mode shall be damped. Partial coverage can lead to higher or lower damping values, therefore generally an increase in shim length does not ultimately lead to a larger dissipation [51].

Damping ratios for both mentioned damping measures from [17] are compared with the original industrial brake shoe in Table 4. It is obvious that due to the composition of the lining material the brake shoe itself shows a relatively high damping potential of approximately 0.7%. Considering the length differences of both variants configuration (b) shows a greater damping ratio than (a) in the range of 0.9–2.1%. Normally it is assumed that a longer shim length contributes to more damping. This isn't the case here. For a detailed insight, the investigations to partial coverage carried out in [51] can be considered, see also [37].

As a conclusion, it can be stated that measures attached on the outer drum surface as well as the brake shoe show a considerable potential for increasing damping. Future tasks might deal with how to bring the integration of such damping measures in line with cooling fins. Mode shapes determined experimentally correspond to those described in literature [31,39]. This will be discussed in detail in Sect. 3.

### 3 Finite-element drum brake model

The Finite-element modeling of the considered drum brake focuses on the fundamental components, i.e. the academic steel drum and the brake shoes including lining. Similar models have been considered in [31,39]. The backing plate usually designed as thin metal component to protect essential drum parts is not part of the modeling process, see also [31]. All components are modeled with a simplified geometry using Abaqus CAE, meaning chamfers, holes etc. are neglected. The aim of this contribution is not to create a detailed model of an existing drum brake mapping all details correctly, but to show how damping can influence the noise behavior of drum brakes in general. Abaqus/Standard serves as solver for executing complex eigenvalue analyses (CEA). The CEA approach will be discussed in detail in Sect. 3.3.

#### 3.1 Modeling

Hexahedral solid elements with a quadratical approach (C3D20) are used for meshing all brake parts.<sup>2</sup> A convergence analysis carried out yield that the drum, the back plate as well as shim components are meshed with an element length of 2 mm. The lining possesses an element length of 1 mm for mapping higher mode shapes accurately and avoiding numerical issues like large distortions. A shim ring with a width of 40 mm and a thickness of 1 mm is attached to the outer surface of the drum via tie-constraint. A detailed view of the model is shown in Fig. 6.

<sup>2</sup> Note that, parts with a more complex geometry have to be partitioned first when using the hexagonal element type in Abaqus.

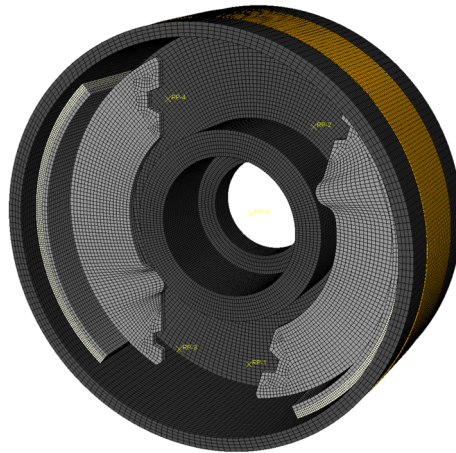


**Fig. 6** FE drum brake model

**Table 5** Lining material parameters

$\rho_1$ $\text{kg m}^{-3}$	$E_1, E_2$ $\text{N mm}^{-2}$	$E_3$ $\text{N mm}^{-2}$	$G_{12}$ $\text{N mm}^{-2}$	$G_{13}, G_{23}$ $\text{N mm}^{-2}$	$\nu_{12}$	$\nu_{13}$	$\nu_{23}$
2600	16000	5500	6500	3000	0.1	0.5	0.5

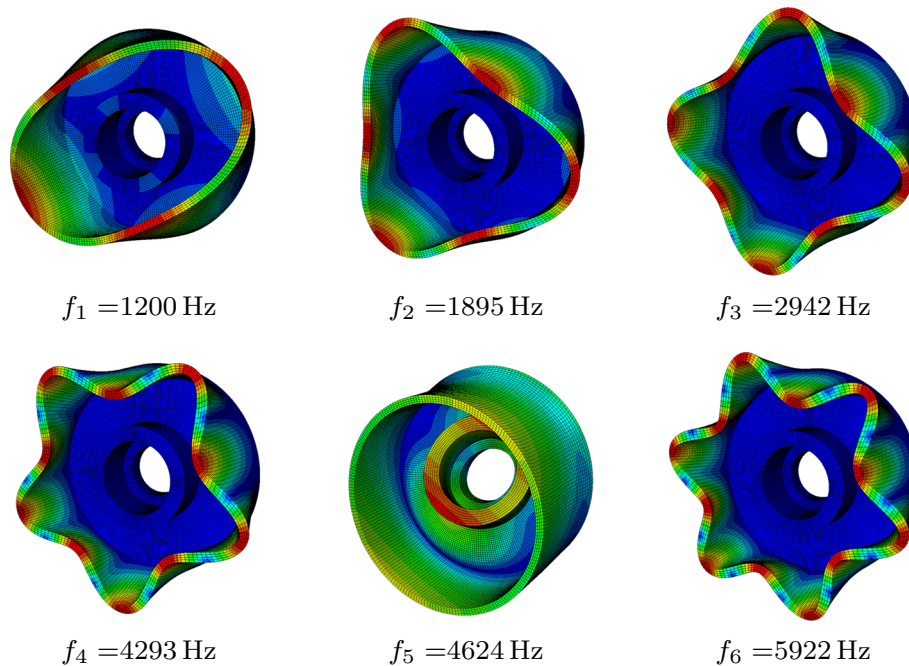
Five reference points (RP-0 to RP-4) positioned near the brake shoes and the center of the drum allow the application of concentrated forces and the bearing (pinned-pinned) as well as pivot of the brake parts. For realizing a simplex or duplex drum brake one brake shoe is mirrored and the force has to be adjusted to the corresponding reference point. The RPs are coupled with beam elements to surface areas of the brake shoe to enable a certain elasticity. The contact between lining and drum is based on a surface to surface formulation considering a contact behavior including tangential forces specified by the friction coefficient. The lining is attached to the back plate by using a tie-constraint.

Steel components like drum and back plate are modeled using isotropic properties such as: density  $\rho_s = 7850 \text{ kg m}^{-3}$ , Young's modulus  $E_s = 210,000 \text{ N mm}^{-2}$  and Poisson ratio  $\nu = 0.3$ . For modeling shims a homogenization approach is used. Previous investigations in [51] showed that shim layer thicknesses of one tenth of a millimeter considering only a coarse mesh can lead to element distortions during computation when modeling each layer separately. These distortions result in numerical issues interpreted wrongly as potential squeal frequency. Therefore, meshing shim structures with a much more appropriate aspect ratio is preferred. A homogenization approach as done in [51] is used combining essential layers of the shim and providing equivalent system properties. The objective is to achieve equivalent system properties of the multi-layer CLD structure by just using one layer in the FE model. The homogenization method for a CLD assembly used is based on the approaches from Nashif et al. [45] and Ross et al. [48]. It has been developed for a classical three-layer structure consisting of a thick beam, a viscoelastic core and a stiff constraining layer. Using this method for brake backplates in disk brakes has delivered good results [51]. After the homogenization the natural frequencies as well as the mode shapes match with a conventional multi-layer compound. Using the theory in [48] the result is a homogenized stiffness parameter used for subsequent FE-simulations. The theory was originally developed for a rectangular cross sections. Due to a more complex geometry of pad back plates and drum, more iterations are needed to achieve a comparable match with experimental results. The Young's modulus for the drum-shim compound has been accordingly adjusted to  $E_{\text{drum}} = 193,000 \text{ N mm}^{-2}$  and the shoe-shim compound to  $E_{\text{shoe}} = 190,000 \text{ N mm}^{-2}$  to map natural frequencies more accurately.

The lining consisting of several components [54] shows a nonlinear and transversal isotropic material behavior [63,68]. There is an anisotropy, meaning that characteristics in out of plane direction are different than in in-plane direction [55]. A deeper insight in this topic is given e.g. in [25,30]. Generally direction-dependent parameters for the friction material are implemented using engineering constants. Common parameters used are listed in Table 5. These parameters implemented for the investigated drum brake are modified parameters based on the data from a previous disk brake model [51].

**Table 6** Natural frequency comparison of FE drum and experiments

	$f_1$ Hz	$f_2$ Hz	$f_3$ Hz	$f_4$ Hz	$f_5$ Hz	$f_6$ Hz
Test	1247	1914	2918	4252	4761	5839
FE	1200	1895	2942	4293	4624	5922

**Fig. 7** FE mode shapes of drum**Table 7** Natural frequency of FE brake shoes and tests, experimental results from [17]

	$f_1$ Hz	$f_2$ Hz	$f_3$ Hz	$f_4$ Hz	$f_5$ Hz	$f_6$ Hz
Test	1431	2301	3148	3383	–	4334
FE	1385	2598	3014	3620	3780	4592

Subsequently six natural frequencies determined from experimental modal analyses and FE-computations are compared in Table 6. Taking a closer look, there is only little deviation considering a simplified geometry neglecting connection holes or chamfers.

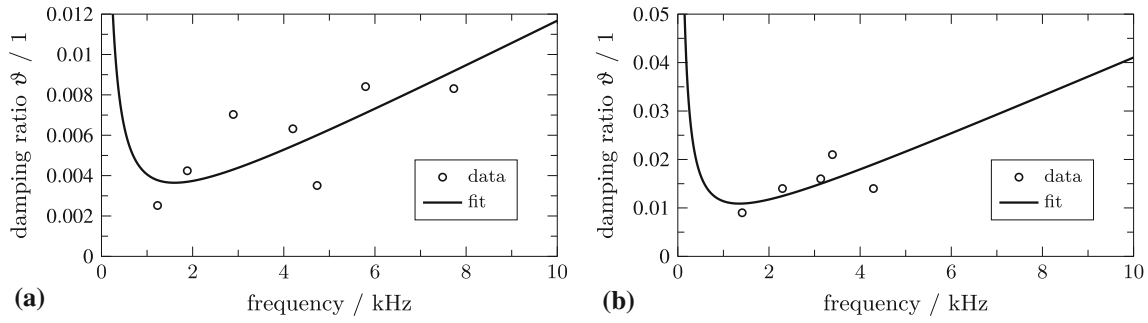
The mode shapes corresponding to the previously shown natural frequencies are listed in Fig. 7.

Table 7 compares measured and computed natural frequencies of brake shoes without using additional damping measures. The computed natural frequency at 3780 Hz could not be determined experimentally. The small discrepancy may result from the geometry used in the FE-model and the unknown lining parameters.

### 3.2 Damping

Damping is often difficult to model and hardly considered or even neglected completely in FE-brake models. One of the most common ways to implement damping mechanism in FE-models is using structural (material) damping. Including frequency-dependent damping characteristics Rayleigh damping is often provided, see [51]. Showing a general influence how the change of damping effects the noise behavior the material damping of the investigated drum is increased successively. For a better modeling quality of measures like shims, damping ratios determined in the previous Sect. 2 are used for subsequent investigations. It should be mentioned that





**Fig. 8** Rayleigh fit: **a** drum with 4 shims ( $139 \times 53\text{mm}^2$ ) and **b** brake shoes with 4 shims ( $50 \times 20\text{mm}^2$ )

component-related damping cannot be transferred exactly to the damping behavior of the entire structure, since often different boundary conditions prevail. For structural damping a complex stiffness matrix using the damping parameter  $\beta_s$ , which is supposed to represent the dissipation properties of the material is essential. The equations represent linear differential equation systems,  $\mathbf{q}$  describes the displacement vector as a function of time,  $\mathbf{M}$  the mass matrix,  $\mathbf{K}$  the stiffness matrix, and  $\mathbf{f}$  the excitation vector. The equation of motion for structural damping is

$$\mathbf{M}\ddot{\mathbf{q}} + \mathbf{K}(1 + i\beta_s)\mathbf{q} = \mathbf{f}. \quad (1)$$

In Rayleigh damping formulation the parameters  $\alpha$  and  $\beta$  are determined from at least two experimentally determined damping ratios of different frequencies. This type of damping represents a purely mathematical construct that weights the influence of the mass and stiffness matrices. The damping matrix  $\mathbf{D}$

$$\mathbf{D} = \alpha \cdot \mathbf{M} + \beta \cdot \mathbf{K} \quad (2)$$

is represented as a linear combination of the mass matrix  $\mathbf{M}$  and the stiffness matrix  $\mathbf{K}$  and allows modal decoupling [9]. The differential equation system to be solved takes the following form

$$\mathbf{M}\ddot{\mathbf{q}} + (\alpha\mathbf{M} + \beta\mathbf{K})\dot{\mathbf{q}} + \mathbf{K}\mathbf{q} = \mathbf{f}. \quad (3)$$

The frequency-dependent relationship between damping ratios  $\vartheta_i$  and angular frequency  $\omega_i$  characterizes

$$\vartheta_i = \frac{\alpha + \beta\omega_i^2}{2\omega_i}. \quad (4)$$

Figure 8 visualizes the fitting process for drum and brake shoes attached with rectangular shims according to the experimental results described in the previous section.

The fits reproduce the course of the measured damping ratios. But there is still a noticeable deviation. To map the measured damping ratios in a more precise way the Caughey series for describing damping also called extended Rayleigh damping might be used [11, 12]. Therein, the general conditions under which a damped dynamic system possesses classical normal modes are specified. Therefore, a proportional Caughey damping matrix  $\mathbf{D}_c$  can be written as follows

$$\mathbf{D}_c = \mathbf{M} \sum_b a_b [\mathbf{M}^{-1} \mathbf{K}]^b. \quad (5)$$

Based on the measured damping ratios  $\vartheta_n$  and corresponding eigenangular frequencies  $\omega_n$  the coefficients  $a_b$  in

$$\vartheta_n = \frac{1}{2 \cdot \omega_n} \sum_b a_b \cdot \omega_n^{2b} \quad (6)$$

can be evaluated exactly [16], in the case that the number of terms matches the number of measured damping ratios. Figure 9 compares Caughey fits considering a different amount of terms, where the coefficients  $a_b$  are chosen such, that an optimum for Eq. (6) is achieved. The two term configuration correspond to the previously shown Rayleigh fits.

With an increasing number of terms the data match can be improved within the measured frequency range. Depending on how many terms are considered for the fitting procedure the behavior at the border areas may show an insufficient and non-physical outcome. The Rayleigh-fit (2-term-fit) shows an adequate representation

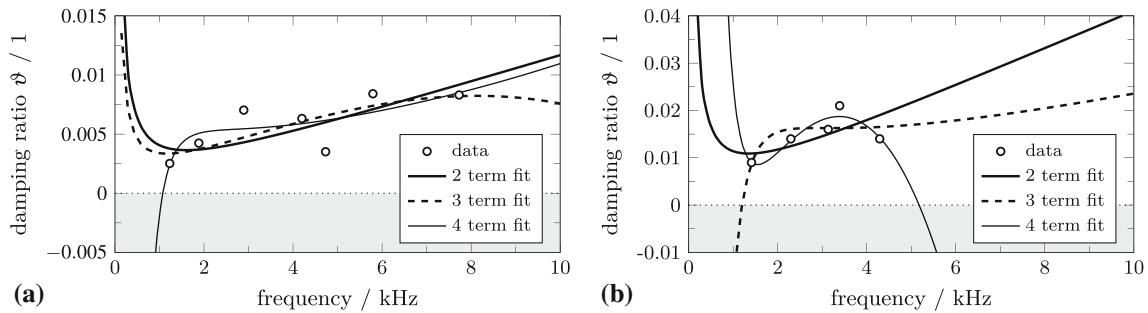


**Fig. 9** Caughey fit comparison: **a** drum with 4 shims ( $139 \times 53\text{mm}^2$ ) and **b** brake shoes with 4 shims ( $50 \times 20\text{mm}^2$ )

of the damping for the further proceeding, particularly for the brake shoe damping above 5 kHz. A general statement that a more precise mapping can be achieved by using the Caughey approach is therefore difficult. This depends strongly on the data measured and a higher term approach may lead, as observed here, to partially unphysical results.

Added to this, that measuring damping is often difficult to reproduce. In [38] it is mentioned that single measurements of composite structures can show very high deviations, partly above 20%. Similar discrepancies were also found in [51]. The test method described in [7] shows that the measured shear modulus contributes to large deviations. Deviations of up to 45% are mentioned.

Therefore, it is often not possible to determine damping ratios for mode shapes exactly. The model is intended to show where damping is particularly effective, see similar investigations in [64] regarding disk brakes. The approach of this contribution is rather to implement damping in a FE brake model in a realistic manner. The Rayleigh parameters are implemented in all shim components as well as the drum and brake shoes acting together as constrained layer damping mechanism.

### 3.3 Complex eigenvalue analysis

Complex eigenvalue analyses (CEA) offer the possibility to generate reproducible results as well as to vary system parameters independently from each other and are therefore often used to provide a rapid assessment. As described in [25] positive real parts do not necessarily mean that a squealing event occurs. Since one positive real part of an eigenvalue indicates an unstable trivial solution, all eigenvalues possessing a positive real part are seen as an indicator for a potential squealing frequency. Due to skew-symmetric circulatory matrix resulting from the non-conservative frictional forces between lining and drum the linearized model has the ability to include eigenvalues with positive real parts [32,44].

It is common practice in the automotive industry, that CEAs are carried out to evaluate the squealing behavior of friction brakes. For all CEAs the model visualized in Fig. 6 is used. This standard practice is divided into four main steps and described in more detail in e.g. [35,40], see also [25]:

- Nonlinear static contact analysis, application of pressure on both brake shoes
- Nonlinear static analysis, computation of friction forces by considering drum rotation (Coulomb friction)
- Normal mode extraction, linearisation at the previous computed equilibrium position; dimension reduction of the linearized system by considering the normal modes of the **MK**-system.
- Complex eigenvalue analysis, computation of eigenvalues and eigenvectors considering the circulatory matrix **N**, the gyroscopic matrix **G** besides damping effects (**MDGKN**-system)

The real part of eigenvalues describes the system damping for a specific vibration mode, the imaginary part the angular frequency, in case of a positive real part its squealing frequency. Positive real parts in the CEA procedure are interpreted that corresponding mode shapes of the brake system are involved in generating noise [62].

For all investigations the duplex brake model in Fig. 6 with and without shims is considered in the frequency range up to 10 kHz. Firstly, a general influence of system parameters like friction coefficient  $\mu$ , pressure  $p$  and speed  $v$  is investigated. As expected, an increase of the friction coefficient favors greater positive real parts for a high amount of eigenvalues. As mentioned in [42] the most important component for noise radiation is the brake drum. The material damping of the drum is varied to show how an increase of damping effects the real

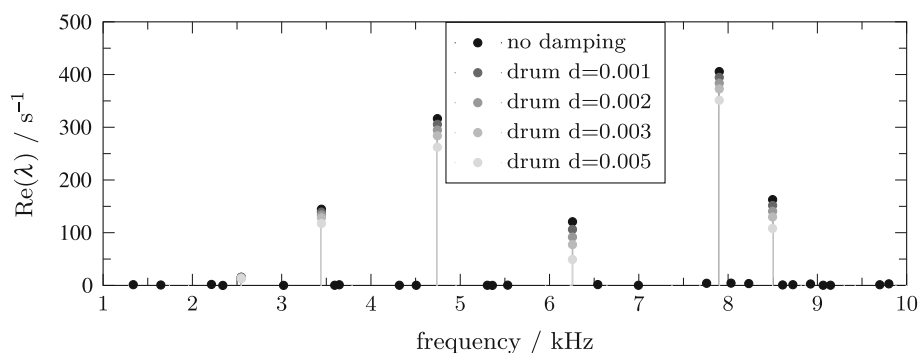


**Fig. 10** Material damping variation of brake drum

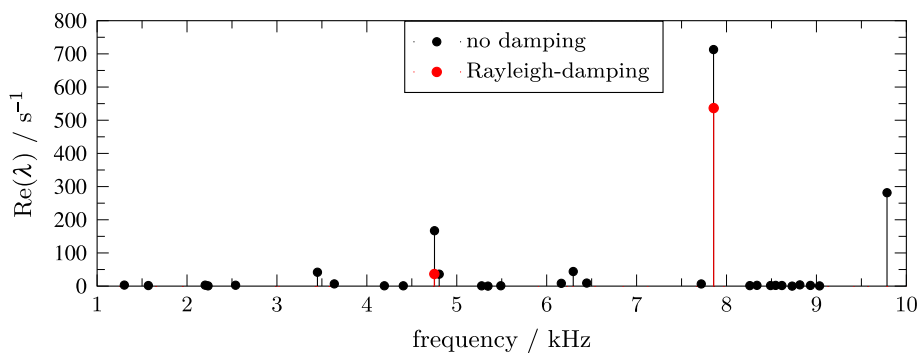


**Fig. 11** Rayleigh-damping included in brake drum

parts of the computed eigenvalues  $\text{Re}(\lambda)$ . The results of the computations are shown in Fig. 10 for  $\mu = 0.6$ . In this case the FE model does not include any shims, the focus is on increasing the drum damping without using additional components.<sup>3</sup>

It is apparent, that a small amount of damping shifts eigenvalues with small positive real parts in the negative quadrant. When increasing the drum damping the real parts decrease gradually, but there are still eigenvalues possessing a larger positive real part. Note, that an increase of damping exclusively causes a stabilization of the system is inaccurate [29]. Increasing damping can lead to a destabilization of the system, as investigated e.g. in [22].

For a more realistic modeling of damping structures, the Rayleigh parameters  $\alpha$  and  $\beta$  having resulted from the fit in Sect. 3.2 are implemented. The eigenvalues of the drum brake model with a lack of damping is compared with Rayleigh damping in Fig. 11. The shim ring applied on the drum surface shown in Fig. 6 is considered for both configurations, the damped and undamped model, to compare the influence on the eigenvalues directly. In the undamped case, the shim ring only possesses elastic properties.

The computations show that damping the outer surface drum contributes to a significant improvement in noise behavior. The additional drum damping effects that all red marked real parts below 4.5 kHz are negative and therefore not visible in the Figure. Only two eigenvalues show a positive real part in the frequency range between 4.5 and 10 kHz. In addition, a further increase of damping, even though this cannot be attained with a realistic shim damping has been investigated. The damping increase showed that almost all eigenvalues with a positive real part could be shifted successfully to the negative half-plane. However, only two eigenvalues rest in the positive half-plane. A possible explanation for this might be, that their corresponding eigenvectors or mode shapes are not effected by the damping in the added shims. To stabilize all vibrational modes it is therefore necessary to add additional damping in other parts of the brake. To finally assess the squeal behavior of the shown damping measures, dynamometer tests have to be carried out first.

As indicated previously, the brake drum is involved in a large number of relevant mode shapes emitting noise. This confirms Fig. 12 illustrating two relevant drum brake mode shapes. The different boundary conditions

<sup>3</sup> The computation time is roughly 260 min according to finer meshing of the components compared to common industrial models and the transversal isotropic material behavior of the lining.

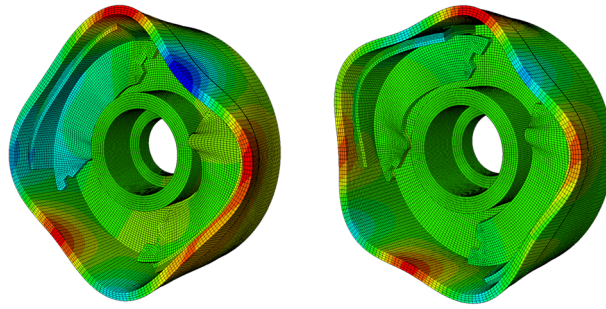


**Fig. 12** Mode shapes of drum brake at 3450 Hz and 4752 Hz

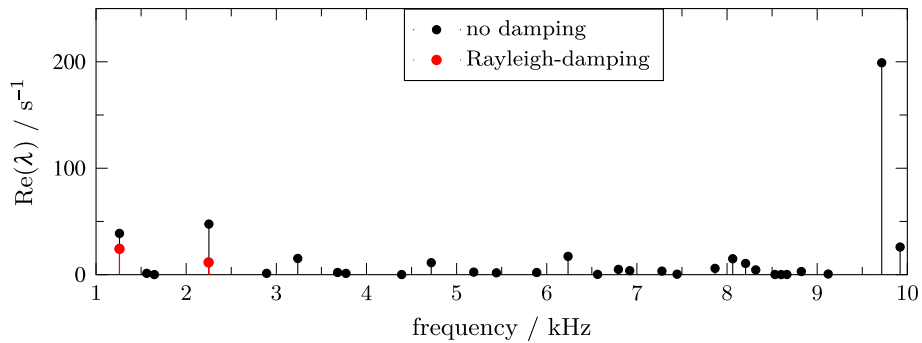


**Fig. 13** Rayleigh-damping included in brake shoes

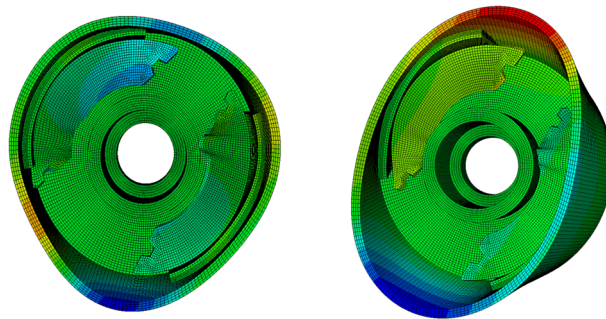


**Fig. 14** Mode shapes of drum brake at 1260 Hz and 2248 Hz

of the drum brake mode shapes (pinned-pinned) do not allow a direct comparison to the free-free supported drum shapes in Fig. 7.

Furthermore, shims are applied on brake shoes as the previously described damping measure (a) in Table 4. The results are summarized in Fig. 13.

This measure shows a high effectiveness in the frequency range above 2.5 kHz. All positive real parts marked in red have been shifted successfully in the negative half-plane and are therefore again not visible in Fig. 13. But there are still two positive real parts in the lower frequency range remaining. As previously shown, Fig. 14 clarifies that the drum and brake shoes are involved in the relevant mode shapes.

## 4 Conclusions

A Finite element drum brake model has been presented investigating how damping measures influence the noise behavior. Experimental modal analysis has been used primarily for determining damping ratios of brake components. Assessing the model shows that natural frequencies as well as damping characteristics of brake components have been mapped sufficiently accurate. The contacts and determined mode shapes behave as expected. While considering the complexity level of the drum brake model brake parts like back plate or

wheel brake cylinders have been neglected. The claim was rather to investigate whether damping measures can improve the noise behavior of drum brakes. Shims applied to the outer drum surface as well as the brake shoes improve the noise behavior significantly. Therefore, it can be stated that damping the drum and brake shoes are one of the key aspects for reducing or even preventing squeal in the future. A combination of both measures should be aimed to achieve silent drum brakes. Note that additional masses and the overall stiffness influence the entire brake system.

One reason why positive real parts still occur despite damping measures could be, that the composites applied are effective only for bending mode shapes. As mentioned in [28] for torsional modes there was a lower effectiveness shown due to a small angular displacement. Currently measures in disk brake system are investigated and tested very extensively. Nevertheless, such measures can play an important role in drum brakes soon.

A next step will be the validation of the presented FE drum brake model. Therefore, measurements of a dynamometer test rig are performed.

**Acknowledgements** This work is funded by the Deutsche Forschungsgemeinschaft (DFG, German Research Foundation) SPP1897 “Calm, Smooth, Smart - Novel approaches for influencing vibrations by means of deliberately introduced dissipation”, WA 1427/27-2, Project Number 314964071 “Suppressing brake vibrations by deliberately introduced damping”. The authors would like to acknowledge AL-KO Kober SE for providing brake parts and Wolverine Advanced Materials for providing damping materials.

**Open Access** This article is licensed under a Creative Commons Attribution 4.0 International License, which permits use, sharing, adaptation, distribution and reproduction in any medium or format, as long as you give appropriate credit to the original author(s) and the source, provide a link to the Creative Commons licence, and indicate if changes were made. The images or other third party material in this article are included in the article’s Creative Commons licence, unless indicated otherwise in a credit line to the material. If material is not included in the article’s Creative Commons licence and your intended use is not permitted by statutory regulation or exceeds the permitted use, you will need to obtain permission directly from the copyright holder. To view a copy of this licence, visit <http://creativecommons.org/licenses/by/4.0/>.

**Funding** Open Access funding enabled and organized by Projekt DEAL.

## Declarations

**Conflict of interest** The authors declare that they have no conflict of interest.

## References

1. Abdulridha, M.F., Jusoh, M.A., Abu Bakar, A.R., Abdullah, M.R.: Reduction of drum brake squeal noise using constrained layer damping (CLD). *Jurnal Teknologi* **79**(7–4), 1–4 (2017)
2. Abdullah, M.A., Abdul Rahim, E., Abu Bakar, A.R., Akop, M.Z.: Numerical analysis of the effectiveness of brake insulator in decreasing the brake squeal noise. *J. Mech. Eng. Technol.* **9**(1), 87–102 (2017)
3. Abd Rahman, M.R., Vernin, G., Abu Bakar, A.R.: Preventing drum brake squeal through lining modifications. *Appl. Mech. Mater.* **471**, 20–24 (2014)
4. AbuBakar, A., Sharif, A., Rashid, M., Ouyang, H.: Brake squeal: complex eigenvalue versus dynamic transient analysis. SAE Technical Paper 2007-01-3964 (2007)
5. Ahmed, I.: Modeling of vehicle drum brake for contact analysis using ansys. SAE Technical Paper 2012-01-1810, 1–13 (2012)
6. Antunes, D.S., Masotti, D., Ferreira, N.F., Neis, P.D., Miguel, L.F.F., Favero, J.: Damping effect on nonlinear drum brake squeal prediction. *J. Braz. Soc. Mech. Sci. Eng.* **44**(97) (2022)
7. ASTM E 756-05: Standard Test Method for Measuring Vibration-Damping Properties of Materials, pp. 1–14 (2005)
8. Baba, S.N.N., Hamid, M.N.A., Soid, S.N.M., Zafelem, M.N., Omar, M.S.: Analysis of drum brake system for improvement of braking performance. In: Öchsner, A. (ed.) *Engineering Applications for New Materials and Technologies, Advanced Structured Materials*, vol. 85, pp. 345–357 (2018)
9. Bathe, K.-J., Wilson, E.L.: *Numerical Methods in Finite Element Analysis*. Prentice-Hall, Upper Saddle River (1976)
10. Breuer, B., Bill, K.H.: *Bremsenhandbuch Grundlagen Komponenten, Systeme, Fahrdynamik*, 5th edn. Springer Vieweg, Wiesbaden (2017)
11. Caughey, T.K.: Classical normal modes in damped linear dynamic systems. *J. Appl. Mech.* **27**(2), 269–271 (1960)
12. Caughey, T.K., O’Kelly, M.E.J.: Classical normal modes in damped linear dynamic systems. *J. Appl. Mech.* **32**(3), 583–588 (1965)
13. Chen, F., Tong, H., Chen, S.E., Quaglia, R.: On automotive disc brake squeal part IV: reduction and prevention. SAE Technical Paper 2003-01-3345, pp. 1–13 (2003)
14. Chen, F.: Disc brake squeal: an overview. SAE Technical Paper 2007-01-0587, pp. 1–17 (2007)
15. Chu, F.H., Wang, B.P.: Experimental determination of damping in materials and structures. In: Torvik, P.J. (ed.) *Damping Applications for Vibration Control*, vol. 38, pp. 113–122. American Society of Mechanical Engineers, Chicago (1980)

16. Clough, R.W., Penzien, J.: Dynamics of Structures, 3rd edn. Computers & Structures, Inc., Berkeley (2003)
17. Conrad, J.: Bestimmung modaler Eigenschaften von Trommelbremskomponenten und Erprobung von Maßnahmen zur Dämpfungserhöhung, Bachelor thesis, MMD, TU Berlin (2019)
18. Cunefare, K.A., Graf, A.J.: Disc brake rotor squeal suppression using dither control. SAE Technical Paper 2001-01-1605, pp. 1–7 (2001)
19. Dias, A.L., Rodrigues, R.d.N., Bezerra, R.d.A., Lamary, P.: Heavy duty automotive drum brake squeal analysis using the finite element method. *J. Vib. Eng. Technol.* (2021)
20. Dias, A.L., Rodrigues, R., da Bezerra, R., Lamary, P.: Automotive simplex and duplex drum brake squeal analysis using the finite element method. *Noise Vib. Worldwide* **53**(1–2), 49–64 (2022)
21. Flint, J.: Disc brake squeal. Ph.D. thesis University of Southern Denmark Engineering College of Odense, Vester Kopi (2002)
22. Fritz, G., Sinou, J.-J., Duffal, J.-M., Jézéquel, L.: Investigation of the relationship between damping and mode-coupling patterns in case of brake squeal. *J. Sound Vib.* **307**(3–5), 591–609 (2007)
23. Ganguly, S., Tong, H., Dudley, G., Connolly, F., Hoff, S.: Eliminating drum brake squeal by a damped iron drum assembly. SAE Technical Paper 2007-01-0592, pp. 1–10 (2007)
24. Graesser, E.J., Wong, C.R.: The relationship of traditional damping measures for materials with high damping capacity: a review. In: Kinra, V.K., Wolfenden, A. (eds.) *M3D: Mechanics and Mechanisms of Material Damping*, pp. 316–343. American Society for Testing and Materials ASTM PCN 04-011690-23, Philadelphia (1992)
25. Gräbner, N.: Analyse und Verbesserung der Simulationemethode des Bremsenquietschens. Ph.D. thesis TU Berlin (2016)
26. Hagedorn, P., Heffel, E., Lancaster, P., Müller, P.C., Kapuria, S.: Some recent results on MDGKN-systems. *ZAMM* **95**(7), 695–702 (2015)
27. Hamabe, T., Yamazaki, I., Yamada, K., Matsui, H., et al.: Study of a method for reducing drum brake squeal. SAE Technical Paper 1999-01-0144 (1999)
28. Hamid, M.N.A., Teoh, C.-Y., Ripin, Z.M.: The operational deflection shapes and transient analysis of the brake shoes in drum brake squeal. *Proc. IMechE Part D J. Automob. Eng.* **227**(6), 866–884 (2013)
29. Hoffmann, N., Gaul, L.: Effects of damping on mode-coupling instability in friction induced oscillations. *ZAMM* **83**(8), 524–534 (2003)
30. Hornig, S.A.: Development of measurement and identification methods for automotive brake lining material properties in NVH relevant loading parameter range. Ph.D. thesis TU Berlin (2015)
31. Huang, J., Krousgrill, C.M., Bajaj, A.K.: Modeling of automotive drum brakes for squeal and parameter sensitivity analysis. *J. Sound Vib.* **289**(1–2), 245–263 (2006)
32. Hultén, J.: Brake squeal—a self-exciting mechanism with constant friction. SAE Technical Paper 932965, pp. 1–11 (1993)
33. Kerwin, E.M., Jr.: Damping of flexural waves by a constrained viscoelastic layer. *J. Acoust. Soc. Am.* **31**(7), 952–962 (1959)
34. Kinkaid, N.M., O'Reilly, O.M., Papadopoulos, P.: Automotive disc brake squeal. *J. Sound Vib.* **267**(1), 105–166 (2003)
35. Kung, S.-W., Stelzer, G., Belsky, V., Bajer, A.: Brake squeal analysis incorporating contact conditions and other nonlinear effects. SAE Technical Paper 2003-01-3343, pp. 1–9 (2003)
36. Kusano, M., Ishidou, H., Matsumura, S., Washizu, S.: Experimental study on the reduction of drum brake noise. SAE Technical Paper 851465 (1985)
37. Lall, A.K., Asnani, N.T., Nakra, B.C.: Vibration and damping analysis of rectangular plate with partially covered constrained viscoelastic layer. *J. Vib. Acoust. Stress. Reliab. Des.* **109**(3), 241–247 (1987)
38. Laboratory measurement of the composite vibration damping properties of materials on a supporting steel bar. SAE Technical Paper J1637 (1993)
39. Lee, J.M., Yoo, S.W., Kim, J.H., Ahn, C.G.: A study on the squeal of a drum brake which has shoes of non-uniform cross-section. *J. Sound Vib.* **240**(5), 789–808 (2001)
40. Lin, S.C., Guan, C.C., Abu Bakar, A.R., Jamaluddin, M.R., Harujan, W.M.M.W., Ghani, B.A.: Disc brake squeal suppression through chamfered and slotted pad. *Int. J. Veh. Struct. Syst.* **3**(1), 28–35 (2011)
41. Mead, D.J.: *Passive Vibration Control*. Wiley, Chichester (2000)
42. Miha, P., Grega, O., Iztok, P., Matjaž, Š.: Detailed analysis of drum brake squeal using complex eigenvalue analysis. *J. Vibroeng.* **15**(3), 1365–1377 (2013)
43. Moreira, R.A.S., Rodrigues, J.D.: Partial constrained viscoelastic damping treatment of structures: a modal strain energy approach. *Int. J. Struct. Stab. Dyn.* **6**(3), 397–411 (2006)
44. Müller, P.C.: *Stabilität und Matrizen Matrizenverfahren in der Stabilitätstheorie linearer dynamischer Systeme*. Springer, Berlin (1977)
45. Nashif, A.D., Jones, D.I.G., Henderson, J.P.: *Vibration Damping*. Wiley, Chichester (1985)
46. Ouyang, H., Nack, W., Yuan, Y., Chen, F.: Numerical analysis of automotive disc brake squeal: a review. *Int. J. Veh. Noise Vib.* **1**(3–4), 207–231 (2005)
47. Phatak, A., Kulkarni, P.: Drum brake backplate analysis and design modification to control squeal noise. *Int. J. Eng. Dev. Res.* **5**(3), 920–928 (2017)
48. Ross, D., Ungar, E.E., Kerwin, E.M., Jr.: Damping of plate flexural vibrations by means of viscoelastic laminae. In: Ruzicka, J.E. (ed.) *Structural Damping*, pp. 49–87. Pergamon Press, New York (1959)
49. Schmid, D.: Constrained-layer-damping shear bending. figshare. [https://figshare.com/articles/Constrained-layer-damping\\_shear\\_bending/8143808](https://figshare.com/articles/Constrained-layer-damping_shear_bending/8143808), license CC BY4.0 (2019). <https://doi.org/10.6084/m9.figshare.8143808.v1>
50. Schmid, D., Sessner, V., Gräbner, N., von Wagner, U., Weidenmann, K.A.: Parameter identification of brake pad shims for complex eigenvalue analysis. *Proc. Appl. Math. Mech.* **19**(1), 1–4 (2019)
51. Schmid, D.: Zum Einfluss von Dämpfung auf Bremsenschwingungen. Ph.D. thesis TU Berlin (2020)
52. Schmid, D.: Non-industrial steel drum. figshare. Figure, [https://figshare.com/articles/figure/Non-industrial\\_steel\\_drum/17714888](https://figshare.com/articles/figure/Non-industrial_steel_drum/17714888), license CC BY4.0 (2022). <https://doi.org/10.6084/m9.figshare.17714888.v1>
53. Schmid, D.: Modal analysis set-up of non-industrial steel drum. figshare. Figure. [https://figshare.com/articles/figure/Modal\\_analysis\\_set-up\\_of\\_non-industrial\\_steel\\_drum/17715890](https://figshare.com/articles/figure/Modal_analysis_set-up_of_non-industrial_steel_drum/17715890), license CC BY4.0(2022). <https://doi.org/10.6084/m9.figshare.17715890.v1>

54. Selamat, M.S.B.: Friction materials for brakes application. *J. Ind. Technol.* **14**(2), 9–25 (2005)
55. Shi, T.S., Dessouki, O., Warzecha, T., Chang, W.K., Jayasundera, A.: Advances in complex eigenvalue analysis for brake noise. *SAE Technical Paper* 2001-01-1603, pp. 1–7 (2001)
56. Soovere, J., Drake, M.L.: Aerospace structures technology damping design guide volume 1—technology review. *AFWAL-TR-84-3089* (1985)
57. Suzuki, Y., Ohno, H.: A study on drum-brake noise of heavy duty vehicle. *SAE Technical Paper* 811399 (1981)
58. Teoh, C.-Y., MohdRipin, Z.: Dither effect on drum brake squeal. *J. Vib. Control* **23**(7), 1057–1072 (2015)
59. Ungar, E.E.: Structural damping. In: Beranek, L.L., Vér, I.L. (eds.) *Noise and Vibration Control Engineering—Principles and Applications*, pp. 451–481. Wiley, New York (1992)
60. Vey, C.: Brake systems 2025—future trends. In: Pfeffer, P.E. (ed.) *9th International Munich Chassis Symposium 2018*. Springer, Heidelberg (2019)
61. von Wagner, U., Schlagner, S.: On the origin of disk brake squeal. *Int. J. Veh. Des.* **51**(1–2), 223–237 (2009)
62. Wagner, N., Gaul, L.: Das Phänomen Bremsenquietschen aus der Sicht der Eigenwertanalyse. In: *VDI-Berichte, VDI Schwingungstagung: Modalanalyse und Identifikation; Verfahren und Anwendungen bei dynamischen Systemen*, pp. 373–388 (2004)
63. Wallaschek, J., Hach, K.-H., Solz, U., Mody, P.: A survey of the present state of friction modelling in the analytical and numerical investigation of brake noise generation. In: *Proceedings of the ASME Vibration Conference DETC99/VIB-8357*, pp. 1–12 (1999)
64. Wehner, J.-H., Jekel, D., Sampaio, R., Hagedorn, P.: Damping optimization in simplified and realistic disc brakes. In: *Springer Briefs in Applied Sciences and Technology*, pp. 1–50 (2018)
65. Wickert, J.A., Akay, A.: Damper for brake noise reduction (brake drums). United States Patent, Patent number 6112865, Sept 5, 2000
66. Wolverine Advanced Materials: Shim datasheet (2016)
67. Yang, M., Afaneh, A.-H., Blaschke, P.: A study of disc brake high frequency squeals and disc in-plane/out-of-plane modes. *SAE Technical Paper* 2003-01-1621, pp. 1–11 (2003)
68. Yuhas, D.E., Ding, J., Venkatesan, S.: Non-linear aspects of friction material elastic constants. *SAE Technical Paper* 2006-01-3193, pp. 1–10 (2006)